

Influence of Vanadium Substitution on Phase Structure, Magnetic and Dielectric Properties of BiFeO₃ Ceramics

Qiang Li, Shengxiang Bao*, Tao Hong, Libo Ai, Yingli Liu, Yulan Jing, and Jie Li

State Key Laboratory of Electronic Thin Films and Integrated Devices, University of Electronic Science and Technology of China, Jianshe North Street Chengdu 610054, Sichuan, PR China

(Received 10 December 2017, Received in final form 1 March 2018, Accepted 14 March 2018)

BiFe_{1-x}V_xO₃ (x = 0.00, 0.03, 0.05, 0.07, 0.09) ceramics were prepared by solid-state reaction method. The effect of V⁵⁺ substitution on phase structure, morphology, magnetic and dielectric properties had been investigated. The Rietveld refinement of the X-Ray diffraction data from the BiFe_{1-x}V_xO₃ (BFVO) ceramics showed samples with rhombohedral structure (R3c) for x = 0.00-0.07. When x = 0.09, partial phase structural be translated to orthorhombic phase (Pnma). Morphology showed two kinds of crystal and proved the phase to be transition. Magnetic measurements exhibited weak ferromagnetic behavior of sample. BiFe_{0.93}V_{0.07}O₃ ceramic exhibited the highest value of saturation magnetization. Due to V⁵⁺ substitution, maybe BFVO attributed weak ferromagnetism to structure distortion and phase transition. Dielectric constant kept a stable value in a wide range frequency of 1 MHz to 1 GHz. With V⁵⁺ ions increasing, dielectric constant increased significantly, while dielectric loss kept a low value. These results indicated that BFVO may be promising for application in magneto-electric devices.

Keywords : BiFeO₃ ceramics, V⁵⁺ substitution, phase transition, magnetic, dielectric

1. Introduction

Multiferroic material is a new type multifunctional material with coupled electric, magnetic and structure order parameters. Ferromagnetism material needs to translate metal ions with partially filled orbital, ferroelectricity material needs to translate metal ions with d⁰ electronic configuration [1]. Hence, magneto-electric multiferroic materials both ferroelectric and ferromagnetic ordering within a single phase are rare. As a representative, BiFeO₃ is one of the few materials that possess magneto-electric properties at room temperature, with the space group R3c, a ferroelectric Curie temperature of 820 °C, and an anti-ferromagnetic Néel temperature of 370 °C [2].

BiFeO₃ has attracted much attention due to its potential applications in new type information storage, magnetic sensors and new magneto-electric components. However, BiFeO₃ is limited for device application because it is still many inherent problems to be overcome, such as larger leakage current, weak ferromagnetism and small remnant

polarization. Some studies proved that the properties of BiFeO₃ could be improved by modifying the A-site Bi³⁺ ions or B-site Fe³⁺ ions [3, 4]. In these reports, the transition element substituted at the B-site had been proved to be an effective method on improving magnetic and dielectric properties [5].

Vanadium belongs to the family of transition metal and has high valence of cation. V⁵⁺ has smaller ionic valence than that of Fe³⁺/Fe²⁺, changing the statistical distribution of Fe³⁺/Fe²⁺ as a result of charge compensation, which maybe do suppress the produce of oxygen vacancy. Oxygen vacancy in BiFeO₃ is the major origin in the leakage current and deterioration of insulation [6]. V⁵⁺ is also a higher valence cation than Fe³⁺. It is highly expected that V⁵⁺ substitution for Fe³⁺ could reduce the leakage current and improve the magnetic and dielectric properties.

Several groups had reported partial substitution of Fe³⁺ with V⁵⁺ ions. Priyanka Godara and Reetu Dahiya et al. reported the change of magnetic and dielectric properties with the co-doped with Ba (Sr) and small amount of V. Rietveld refinement studies showed that all samples (Bi_{0.8}Ba_{0.2}Fe_{1-x}V_xO₃, x = 0.0-0.04, Bi_{0.85}Sr_{0.15}Fe_{0.97}V_yO₃, y = 0.0-0.05) had rhombohedral structure [7, 8]. Benfang

©The Korean Magnetism Society. All rights reserved.

*Corresponding author: Tel: +86-13880660992

Fax: +86-028-83206669, e-mail: sxbao@uestc.edu.cn

Yu *et al.* reported that the electrical properties were improved with the co-doped with La and V [9].

So far, few articles had been reported on synthesis, phase transition and improving properties of V⁵⁺ ions substituted BiFeO₃ ceramics. Especially investigation on single V⁵⁺ ion doping have not been reported to date, rather than co-doping in bulk BiFeO₃. Therefore, the main aim of the paper is to study the influence of single V⁵⁺ ion on phase transition, morphology, magnetic and dielectric properties of BiFeO₃ ceramics.

2. Experimental

BiFe_{1-x}V_xO₃ is prepared through conventional solid-state reaction method. The x value was varied as x = 0.00, 0.03, 0.05, 0.07 and 0.09. The stoichiometric amounts of analytical grade powders of Bi₂O₃, Fe₂O₃ and V₂O₅ were weighed, ball milled for 12 h in deionized water, and then dried. The dried mixtures were pre-sintered at 700 °C for 2 h, milled again for 6 h and sintered at 825 °C for 30 min. Finally, the powders were washed by diluted HNO₃ and mixed with polyvinyl alcohol (PVA, 10 % amount) as a binder. The granulated powders were pressed into disk shapes (Ø 18 mm × 8 mm) at 20 MPa, which were sintered at 825 °C for 10 min in air.

XRD spectra were recorded on the X-ray diffractometer (D/max 2400, Rigaku, Tokyo Japan) at room temperature with Cu-K α radiation ($\alpha = 1.5418$ Å) in Bragg-Brentano geometry. The phase and structure analysis were carried out by using Rietveld refinement method through a software GSAS. Microstructural analyses were carried out by using a Scanning Electron Microscope (SEM) (JSM 6490LV, JEOL, Tokyo Japan). Magnetization hysteresis loops were measured by using a Vibrating Sample Magnetometer (VSM) (BHV-525, Riken Denshi, Tokyo Japan). Dielectric behavior was determined by using a HP-4291B RF Impedance Analyzer. Bulk density was measured by using an Auto Density Tester (ADT) (GF-300D, AND Co.) by Archimedes' principle.

3. Results and Discussions

Figure 1 showed the X-ray diffraction patterns of BFVO ceramics. All the diffraction peaks matched with the standard Card (ICCD, JCPDF No. 20-0169) for BiFeO₃. It had been observed that all the samples did not show any impurity phase after being washed by diluted HNO₃. These impurity phases were Bi₂Fe₄O₉ and Bi₂₅FeO₃₉, that they had been observed in metastable BiFeO₃ ceramics due to its chemical kinetics of formation [1]. The transformational process of BiFeO₃ was followed,

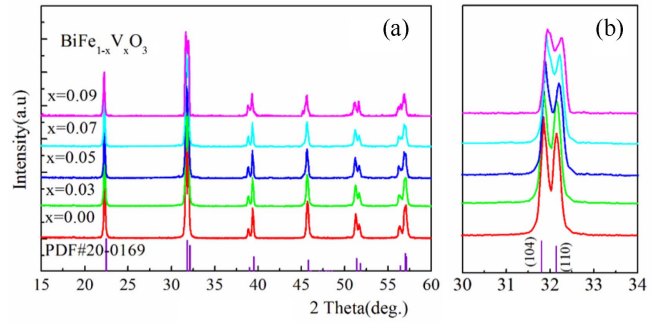
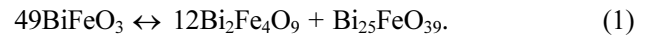


Fig. 1. (Color online) (a) XRD patterns of BFVO ($x = 0.00-0.09$) ceramics at room temperature. (b) Magnified XRD patterns in the vicinity of $2\theta = 32^\circ$ corresponding to (104)/(110) planes.



Hence, in the process of synthesis, Bi₂O₃ and Fe₂O₃ almost reacted to produce BiFeO₃, but still produced a little impurity phases. The method of the washing with dilute HNO₃ had been adopted to remove impurity phase. Perovskite-type BiFeO₃ has a rhombohedrally distorted structure described by R3c space group. In this structure, ferroelectric properties of BiFeO₃ were mainly derived from the hybridization between the arc of 6s² long pair electrons from Bi atom and the 2p orbital electrons of O atom. The magnetic properties were mainly derived from partially filled 3d orbital of Fe atom. Bi³⁺ ions occupy the cubo-octahedral positions, Fe³⁺ ions occupy the octahedral coordination. These cations are displaced from their center of symmetry along [111]_p direction with anions sub lattice having distortion according to an $\bar{a}^+ \bar{a}^- \bar{a}^-$ tilt system [2]. As showed from Fig. 1(a), the relative intensity of diffraction peaks decreased monotonically with increasing of V⁵⁺ ions amount. Interesting, the peak of XRD pattern seemed to shift toward higher angle, which could be observed from Fig. 1(b). This maybe due to the V⁵⁺ (0.54 Å) ions substitution which has smaller ionic radius compared to Fe³⁺ (0.64 Å). Moreover, in order to balance the valence due to the substitution of high valence ions (V⁵⁺), the transformation of Fe³⁺ to Fe²⁺ would be partly occur after oxygen vacancy compensate. Ionic radius of Fe³⁺ (0.64 Å) is less than Fe²⁺ (0.76 Å). In this way, there were three different size ions occupying the B-site, making the sample more distortion. The distortion been produced compressive strain. The compressive strain acted on Fe–O bonds due to fit larger cation (V⁵⁺) into a smaller space, led the deformation of oxygen octahedral and evolution of orthorhombic phase [3].

To study the structural, all samples were analyzed by using Rietveld refinement through a GSAS program.

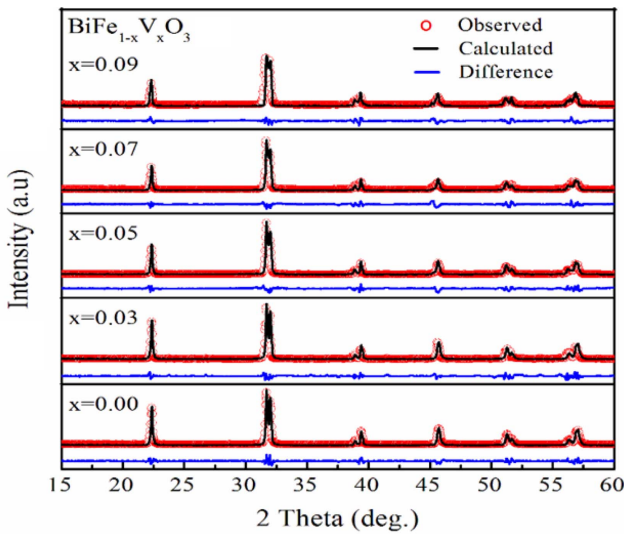


Fig. 2. (Color online) Refined XRD pattern of BFVO ($x = 0.00-0.09$) ceramics.

Figure 2 showed the Rietveld refinement data, including observed, calculated and the different patterns. The results obtained from Rietveld refinement had been summarized in Table 1. Atoms position, scale factor, half-width parameters of all atoms were kept fixed during whole refinement process. The peak shapes were calculated by Pseudo-Voigt function. Good agreement was acquired between the observed and simulated XRD patterns with small χ^2 and R values (i.e., R_{wp} and R_p). The reduction in peak splitting

behavior of (110)/(104) diffraction peaks as showed in Fig. 2(b) and evolution of some tiny peaks, which is a result may be due to the existence crystalline phase both rhombohedral ($R3c$) and orthorhombic ($Pnma$) for $\text{BiFe}_{1-x}\text{V}_x\text{O}_3$ ($x = 0.09$) [4]. Therefore, $\text{BiFe}_{1-x}\text{V}_x\text{O}_3$ ($x = 0.00-0.07$) samples were refined with $R3c$ space group, whereas two phases refinement ($R3c+Pnma$) was refined for $\text{BiFe}_{1-x}\text{V}_x\text{O}_3$ ($x = 0.09$). It was indication that structural modification and symmetry changes brought about by V^{5+} substitution. From Table 1, it showed that there were some changes of atomic coordinates. The reason may be due to the B-site disorder created by the V^{5+} substitution, and changed $\text{Fe(V)}-\text{O}-\text{Fe(V)}$ bond angles, and led to the distortion of FeO_6 . It caused the adjacent two iron atoms relative (111) axis to produce a larger rotation angle, and break part of the incommensurate cycloid spin structure of periodicity 62 nm along $[110]_h$ axis. This would affect the magnetic properties. There was a decrease in $R3c$ cell volume from 373.04 \AA^3 ($x = 0.00$) to 362.12 \AA^3 ($x = 0.09$). It possibly was due to reduction nucleation rate, as a result of the increase in lattice strain inside the lattice caused by ionic size mismatch [5]. The average crystallite size was calculated by using Debye-Scherrer formula,

$$D = K\lambda/\beta\cos\theta, \quad (2)$$

Where D is the crystallite size, K is the Scherrer constant, λ is the wavelength of X-ray, β is FWHM (full width at half maximum) and θ is the diffraction angle. The values

Table 1. Selected structural parameters from Rietveld refinement for BFVO ($x = 0.00-0.09$) ceramics.

Compositions	Crystal structure	Lattice parameters	Atomic coordinates	Fe(V)-O-Fe(V) bond angle	Refinement-density	Bulk density	Refinement-factors (%)
$x = 0.00$	$R3c$ (100 %)	$a=5.5669 \text{ \AA}$ $c=13.8646 \text{ \AA}$ $V=373.04 \text{ \AA}^3$	Bi (0, 0, 0) Fe/V (0, 0, 0.2384) O (0.4991, 0.0589, 0.9430)	98.08	10.073 g/cm ³	7.632 g/cm ³	$R_p=0.107$ $R_{wp}=0.169$ $\chi^2=1.952$
$x = 0.03$	$R3c$ (100 %)	$a=5.5769 \text{ \AA}$ $c=13.8635 \text{ \AA}$ $V=371.42 \text{ \AA}^3$	Bi (0, 0, 0) Fe/V (0, 0, 0.2431) O (0.4392, -0.2732, 0.9545)	88.79	10.404 g/cm ³	7.407 g/cm ³	$R_p=0.160$ $R_{wp}=0.279$ $\chi^2=2.910$
$x = 0.05$	$R3c$ (100 %)	$a=5.5834 \text{ \AA}$ $c=13.8550 \text{ \AA}$ $V=368.44 \text{ \AA}^3$	Bi (0, 0, 0) Fe/V (0, 0, 0.2493) O (0.4023, -0.2374, 0.9498)	82.16	10.836 g/cm ³	7.128 g/cm ³	$R_p=0.166$ $R_{wp}=0.331$ $\chi^2=2.725$
$x = 0.07$	$R3c$ (100 %)	$a=5.5891 \text{ \AA}$ $c=13.8451 \text{ \AA}$ $V=365.09 \text{ \AA}^3$	Bi (0, 0, 0) Fe/V (0, 0, 0.2502) O (0.4002, -0.2316, 0.9445)	80.22	11.209 g/cm ³	7.006 g/cm ³	$R_p=0.176$ $R_{wp}=0.240$ $\chi^2=2.526$
$x = 0.09$	$R3c$ (86.7 %)	$a=5.5945 \text{ \AA}$ $c=13.8377 \text{ \AA}$ $V=362.12 \text{ \AA}^3$	Bi (0, 0, 0) Fe/V (0, 0, 0.2548) O (0.4392, -0.2284, 0.9345)	76.95	11.135 g/cm ³	7.368 g/cm ³	$R_p=0.205$ $R_{wp}=0.282$ $\chi^2=3.177$
	$Pnma$ (13.3 %)	$a=5.5698 \text{ \AA}$ $b=7.9904 \text{ \AA}$ $c=5.5673 \text{ \AA}$ $V=256.346 \text{ \AA}^3$	Bi (0.0365, 0.3057, 0.9704) Fe/V (0.0005, 0, 0.4764) O1 (0.4839, -0.2529, 0.0835) O2 (0.1903, -0.5362, 0.2442)	90.15			$R_p=0.205$ $R_{wp}=0.282$ $\chi^2=3.177$

of D were calculated as 72, 65, 59, 53 and 58 nm for $x = 0.00-0.09$, respectively. The falling of D corresponds to the above date of cell volume. Additional, the bulk density and refinement density were shown in Table 1. With increasing of V^{5+} ions, bulk density showed a trend of first decrease and then increase. However, Refinement density showed an inverse trend. The values of bulk density were measured by Archimedes' principle, which were 7.632, 7.407, 7.128, 7.006, and 7.368 g/cm³, respectively. The values of refinement density were obtained by Rietveld refinement, which were 10.073, 10.404, 10.836, 11.209, 11.135 g/cm³, respectively. This interesting phenomenon can be explained by appearance of pores. Further increase of V^{5+} ions brought more distortion, and led the crystalline shrinkage and increased the refinement density.

The magnetization hysteresis loops of BFVO ceramics were measured up to 5000 Oe at room temperature as shown in Fig. 3. Coercivity (H_c) and Saturation Magnetization (M_s) (@ 5000 Oe) were shown in Fig. 4. Although an enhancement of magnetization was observed with V^{5+} ions increasing in B-sites, the magnetization curves were not really saturated for all samples. In pure BiFeO₃, it could be seen that magnetization varies linearly with the applied magnetic field up to 5000 Oe. Similar magnetization curves were also reported by other authors [6]. In fact, BiFeO₃ is known to be G-type antiferromagnetism having a rhombohedrally distorted structure. Interesting, with V^{5+} ions increasing, which made magnetization increases monotonically, both M_s and H_c showed weak ferromagnetic. M_s were 0.5036 emu/g, 0.8676 emu/g, 1.0880 emu/g, 1.2570 emu/g 1.2061 emu/g for $x = 0.00-0.09$, respectively.

The causes of this phenomenon are multiple. It had not been observed impurity phase in the XRD data. Therefore, a small amount of impurity phases did not have

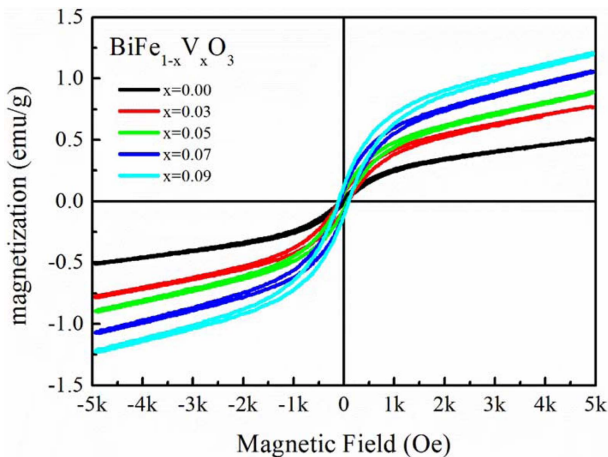


Fig. 3. (Color online) Magnetic hysteresis loops of BFVO ceramics at room temperature ($x = 0.00-0.09$).

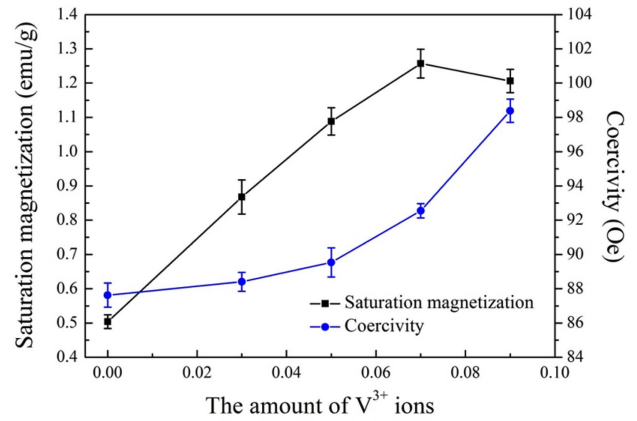


Fig. 4. (Color online) Saturation Magnetization and Coercivity of BFVO depend on V^{5+} ions ($x = 0.00-0.09$).

some effects on magnetic properties. In BiFeO₃, Fe atoms control with the spiral arrangement of spins and directly affect the magnetic properties. Weak spontaneous magnetization was derived from canting of antiferromagnetically ordered Fe-O-Fe spins chain. The appearance of increasing M_s may be due to the change of Fe-O-Fe bond angle by V^{5+} ions substitution. The Rietveld refinement showed that Fe(V)-O-Fe(V) bond angle is 98.08, 88.79, 82.16, 80.22 for $x = 0.00-0.07$, respectively. In case of BFVO ($x = 0.09$) structure changed to a mixed phase structure (86.7 %) rhombohedral ($R3c$) phase and (13.3 %) orthorhombic ($Pnma$) phase. The Fe (V)-O-Fe (V) bond angle of BFVO ($x = 0.09$) changed to 76.95 ($R3c$) and 90.15 ($Pnma$). Thus, V^{5+} ions substitution induce more buckling in Fe(V)-O-Fe(V) bond angle, and finally led to partly collapse of the space modulated spin structure and potential magnetization to be released. These potential magnetization have previously been suppressed in the repetitive spin structure, a period of 62 nm. One other factor, M_s may be related with specific surface area, which increased with the decrease of grain size, and result in more long-range antiferromagnetic order of the particle surface interrupted. The result was responded to the SEM figure. Another factor, the magnetization in BFVO was due to occurring in super exchange interaction between Fe^{2+} and Fe^{3+} ions [7]. BFVO requires charged compensation with the addition of V^{5+} ions, which had been achieved by the transformation of Fe^{3+} to Fe^{2+} or oxygen vacancies decreased. If Fe^{3+} translate, statistical distribution of ions (V^{5+}) in the antiferromagnetic lattice of Fe^{3+} ions may cause resultant magnetism [8].

Like saturation magnetization, the coercivity of all samples showed similar behavior. The variation of H_c of samples increased with the increasing of V^{5+} ions. H_c were 87.624 Oe, 88.402 Oe, 89.538 Oe, 92.551 Oe 98.383

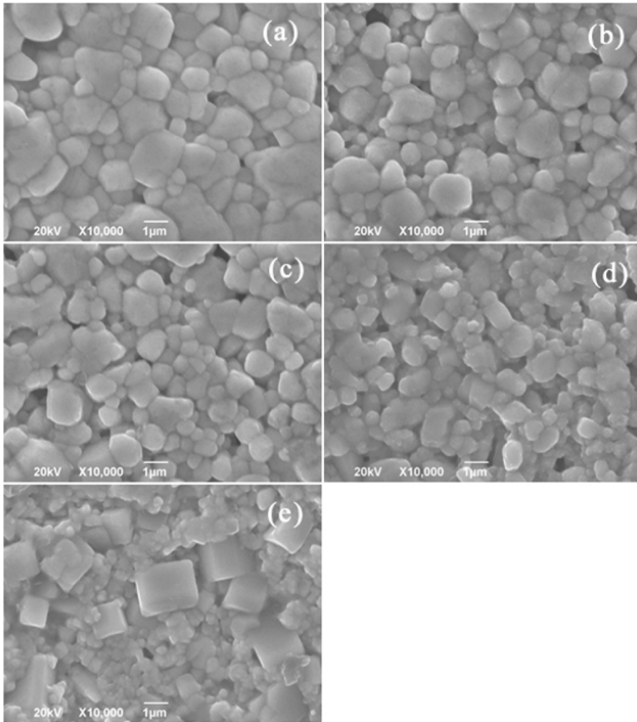


Fig. 5. SEM images of BFVO ceramics, (a) $x = 0.00$, (b) $x = 0.03$, (c) $x = 0.05$, (d) $x = 0.07$, (e) $x = 0.09$.

H_c for $x = 0.00-0.09$, respectively. The main source of H_c for magnetic materials is shaped anisotropy, magneto-elastic anisotropy and magnetocrystalline anisotropy. The particles are spherical in nature, which found in SEM figure below. Thus, the contribution of shape anisotropy in H_c can be neglected. So the observed H_c for all samples may be due to the magnetocrystalline anisotropy and magnetoelastic anisotropy.

The morphology of the BiFeO_3 ceramics was examined using SEM. Typical SEM images were shown in Fig. 5. As it can be seen, V^{5+} ions substitution made smaller grain size and produced some big cuboids. Figure 5(a) showed the size of grains was about $1 \mu\text{m}$ and structure was irregular shapes and non-uniform. Figure 5(b), 5(c) and 5(d) showed gradually the appearance of a few small grains and pores. The reason was that V^{5+} ion substitution lead samples to lattice distortion, and brought in crystalline shrinkage, and produced some small grains and pores. Figure 5(e) showed that it not only appeared small grains but also some big cuboids. The grain and grain boundaries of small grains were not defined and clearly visible. This cuboid was due to the V^{5+} ions substitution led transition of rhombohedral to orthorhombic phase. Meanwhile, The big cuboid balanced space of crystalline shrinkage, and reduced the pores [9].

Figure 6 showed the real part of dielectric constant (ϵ')

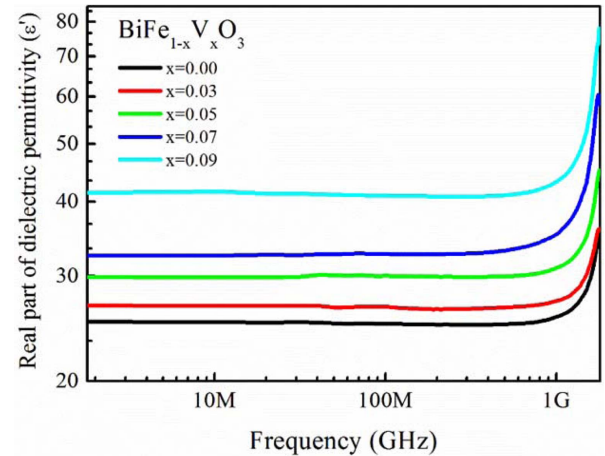


Fig. 6. (Color online) Dielectric permittivity (ϵ') of BFVO ceramics at 1 MHz-1.8 GHz.

as a function of room temperature for all samples in a frequency range 1 MHz-1.8 GHz, and the values of initial ϵ' (@ 1 MHz) was about 25, 26, 29, 32 and 41 for $x = 0.00-0.09$, respectively. From the view of substituting concentration, ϵ' increased with V^{5+} ions increasing. The increasing value of ϵ' might be interpreted in the aspect of the suppression of the oxygen vacancy concentration, which reduced the leak current. The nonstoichiometric oxygen deficiency is an inherent problem with pure BiFeO_3 , according to formula,



Where V_o^x and V_o^{2+} are oxygen vacancy and oxygen position, respectively. Due to V^{5+} ion possesses a higher valence than Fe^{3+} ions, which played a role of donor in BFVO. The addition of V^{5+} to BFVO requires charge compensation, which can suppress the formation of oxygen vacancies [10]. On the other hand, In synthesis process of high temperature sintering, part of the low melting point of Bi^{3+} would evaporate and bring a charge imbalance, leading to increase of free charge and decrease of the value of ϵ' . High valence of V^{5+} ions would suppress the phenomenon and reduce the free charge through compensate the positive charge. Meanwhile, V^{5+} ions would suppress the transformation of Fe^{3+} to Fe^{2+} . The conduction is through exchange of electrons between $\text{Fe}^{2+} \leftrightarrow \text{Fe}^{3+}$ cations on B-sites. In addition, due to the substituting of V^{5+} ions, the inhomogeneous behavior of grain and grain boundary regions led the increase of ϵ' in substitutable samples [11]. From the view of frequency, ϵ' kept stable in a range frequency of 1 MHz-1 GHz. This stabilization will lead sample to potential application.

Figure 7 showed the variations of dielectric loss ($\tan\delta$) versus frequency (1 MHz-1.8 GHz), which was about

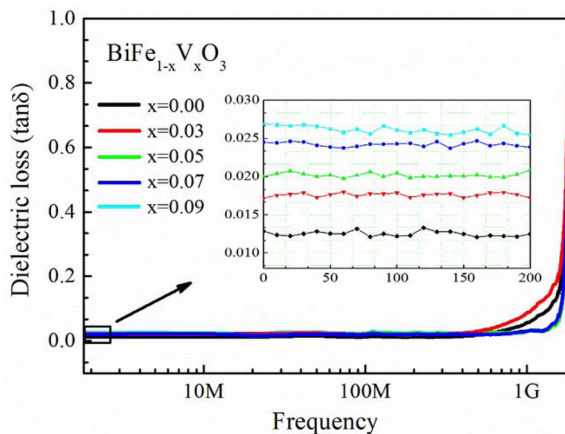


Fig. 7. (Color online) Dielectric loss ($\tan\delta$) of BFVO ceramics at 1 MHz-1.8 GHz.

0.012, 0.017, 0.019, 0.024, 0.026 for $x = 0.00-0.09$, respectively. They were slightly increased and kept stable in a wide range frequency of 1 MHz-1 GHz. The $\tan\delta$ was calculated by using the formulas, and they are one of the most important parameters for engineering applications. According to formula,

$$\tan\delta = \varepsilon''/\varepsilon' \quad (4)$$

The dielectric loss was the energy dissipation in the dielectric system, including conductance leakage loss and slow polarization loss. The dielectric was not an ideal insulator, because there were inevitably generated leakage conductance and conductance leakage loss [12]. It was displayed on the microstructure of samples, macroscopically. As shown in Fig. 5, with the increase of substituting amount, there were more small grains and more pores, which led to increase in the intensity of leakage loss. Slow polarization mainly includes thermionic polarization and hot turning-direction polarization, etc., due to the establishment of a long time (10^{-4} s- 10^{-9} s). When an electric field changes the frequency beyond a certain limit, there will be no time to build these slow polarization and produce the polarization hysteresis. Meanwhile, it will consume part of the energy, form a slow polarization loss. The substitution of V^{5+} would produce grain boundary defects and non-uniform ions, increasing the established time and slowing polarization loss [13]. Although there was a small increase in the dielectric loss with V^{5+} ions, it still maintains a lower value and has potential applications in high frequency.

4. Conclusions

BiFeO₃ with V^{5+} substitution brought about distorted rhombohedral phase ($R3c$), while produced additional

orthorhombic ($Pnma$) phase for BFVO ($x = 0.09$). The substitution driven phase transition was confirmed by XRD and Rietveld refinement. SEM morphology exhibited clear orthorhombic grain growth habit and a smaller estimated particle size. Substitution of V^{5+} increased the further distortions, leading to partly collapse of the space modulated spin structure, which affected grain size and transformation of Fe^{3+} to Fe^{2+} ions, and released the potential magnetic properties in magnetization hysteresis loops. With the increase of V^{5+} ions concentration, the dielectric constant was enhanced and maintained explained on the oxygen vacancies. Meanwhile, dielectric loss had maintain a lower value in a wide frequency.

Acknowledgement

This work was supported by the National Key Research and Development Program of China (No. 2016YFA0300801), and by the National Nature Science Foundation of China (Nos. 51602036, and 51672036), and the key projects of Sichuan Province (Nos. 2017GZ0408 and 2017GZ0415), and the key projects of Chengdu (2016-HM01-00225-SF), and Guizhou province key R&D program [2016]3011.

References

- [1] Q. Li, S. X. Bao, Y. X. Li, L. J. Song, W. Jiang, and Y. D. Hu, *J. Mater. Sci.-Mater. El.* **26**, 8887 (2015).
- [2] P. Godara, A. Agarwal, N. Ahlawat, and S. Sanghi, *J. Mol. Struct.* **1097**, 207 (2015).
- [3] S. Dash, R. N. P. Choudhary, P. R. Das, and A. Kumar, *Appl. Phys. a-Mater.* **118**, 1023 (2015).
- [4] V. A. Khomchenko, I. O. Troyanchuk, T. M. R. Maria, D. V. Karpinsky, S. Das, V. S. Amaral, and J. A. Paixão, *J. Appl. Phys.* **112**, 064105 (2012).
- [5] P. C. Sati, M. Kumar, and S. Chhoker, *J. Am. Ceram. Soc.* **98**, 1884 (2015).
- [6] V. R. Palkar, D. C. Kundaliya, S. K. Malik, and S. Bhattacharya, *Phys. Rev. B* **69**, 212102 (2004).
- [7] D. V. Thang, D. T. X. Thao, and N. Van Minh, *J. Magn.* **21**, 29 (2016).
- [8] S. Godara and B. Kumar, *Ceram. Int.* **41**, 6912 (2015).
- [9] Q. Li, S. Bao, Y. Liu, Y. Li, Y. Jing, and J. Li, *J. Alloy Compd.* **682**, 672 (2016).
- [10] C. Y. Quan, Y. M. Han, N. Gao, W. W. Mao, J. Zhang, J. P. Yang, X. A. Li, and W. Huang, *Ceram. Int.* **42**, 537 (2016).
- [11] P. C. Sati, M. Kumar, S. Chhoker, and M. Jewariya, *Ceram. Int.* **41**, 2389 (2015).
- [12] P. Suresh, P. D. Babu, and S. Srinath, *Ceram. Int.* **42**, 4176 (2016).
- [13] Y. C. Huang, Y. Y. Liu, Y. T. Lin, H. J. Liu, Q. He, J. Y. Li, Y. C. Chen, and Y. H. Chu, *Adv. Mater.* **26**, 6335 (2014).